Processing and Application of Ceramics 13 [2] (2019) 149–156
https://doi.org/10.2298/PAC1902149V

Development of bioactive and biocompatible ceramic composites based on potassium polytitanate

Ángel Villalpando-Reyna[1], Dora A. Cortés-Hernández[1,*], Jose M. Granjeiro[2], Marcelo Prado[3], Alexander V. Gorokhovsky[4], José C. Escobedo-Bocardo[1], José M. Almanza-Robles[1], David Rentería-Zamarrón[5]

[1]*CINVESTAV-Unidad Saltillo, Carretera Saltillo - Monterrey km 13, Apdo. Postal 663, C.P. 25000, Saltillo, Coahuila, México*
[2]*UFF, Universidade Federal Fluminense, Outeiro do São Joao Batista s/n Campus do Valonginho, Centro/Niterói, Brazil*
[3]*IME, Instituto Militar de Engenharia, Praça Gen. Tibúrcio, № 80 Urca, Rio de Janeiro - RJ, Brazil*
[4]*Saratov State Technical University, Saratov, Russia*
[5]*División de Estudios de Posgrado e Investigación. Tecnológico Nacional de México, Instituto Tecnológico de Saltillo, Saltillo, Coahuila, México*

Received 10 October 2018; Received in revised form 28 February 2019; Accepted 15 May 2019

Abstract

Bioactive and biocompatible composites were successfully prepared by reactive sintering of mixtures of a crystalline titanate precursor and 45S5 Bioglass®. The polytitanate/glass precursor ratios were 20/80, 40/60, 60/40 or 80/20 (wt.%). The powder mixtures were uniaxially pressed and heat treated at 1000 °C for 1 h. During sintering, intensive interactions between raw materials occurred. The formed main crystalline phases were: potassium hexatitanate ($K_2Ti_6O_{13}$), calcium titanate ($CaTiO_3$), calcium silicate ($CaSiO_4$) and sodium-calcium silicate ($Na_6Ca_3Si_6O_{18}$). Additionally, a Si-rich glassy phase was also observed. The mechanism of apatite formation indicated that both crystalline and amorphous phases play important roles in this process. A homogeneous apatite layer was formed on Si–OH, Ti–OH-rich interfaces. In vitro bioactivity was assessed using simulated body fluid (SBF K-9). The in vitro cytotoxicity behaviour was evaluated using a human osteoblast-like cells model and compressive strength by ASTM C-773 standard. All the composites demonstrated high bioactivity as cytotoxicity assays indicated a biocompatibility similar to that of the negative control. The samples showed high cell adherence and elongation cell characteristics similar to those observed on biocompatible systems. The compressive strength of the sintered samples decreased as the polytitanate content precursor was increased. The results obtained indicate that these materials are highly promising composites for medical applications.

Keywords: *silicate glasses, potassium titanate, apatite formation, cytotoxicity, cell adhesion*

I. Introduction

Nowadays, ceramics, glasses and glass-ceramics are used for bone repair and joint defects. Among them, bioactive glasses are employed successfully due to their high bioactivity, since they promote apatite formation on their surfaces when they are exposed to biological environment. Bioactive glasses are employed mainly as coatings of bioinert materials [1], as dense pieces were clinically used for the substitution of the middle-ear bone chain and widely studied in the last decade as scaffolds [2,3]. Additionally, they are used in the conformation of bioactive dense composites [4,5]. Nevertheless, glass-containing bioactive composites have not been deeply investigated despite their main advantages, such as their functional or structural properties related to the combination of microstructural characteristics provided by the different components [6].

*Corresponding author: tel: +52 844 437 1296,
e-mail: *dora.cortes@cinvestav.edu.mx*

Titania based composites and porous titanium have been widely studied for biomedical applications [7–9]. Titania has the tendency to adsorb water on its surface leading to the formation of Ti–OH groups. These basic groups were reported to induce apatite nucleation and crystallization on materials in contact with SBF [10].

A crystalline precursor of potassium polytitanate may show a higher reactivity than titania (TiO_2), whose inert properties are well known. As stated in the literature [7,10–14], titanate phases are highly bioactive when they are in the contact with SBF, due to the formation of Ti–OH groups. Due to this fact, among others, a potassium polytitanate precursor was selected for developing the bioactive composites presented in this work.

The semi-crystalline or amorphous potassium polytitanate precursor ($K_2O \cdot nTiO_2$) synthesized by the molten salt method [15] may be considered as a reinforcing material of composites. This is supported by the tendency of potassium polytitanate ($K_2O \cdot nTiO_2$) to crystallize after an additional heat treatment at temperatures higher than 800–850 °C, as fibre-shaped potassium tetra or hexatitanate, depending on the ratio $n = TiO_2/K_2O$ in the original composition [16,17]. The potassium hexatitanate ($K_2Ti_6O_{13}$) is characterized by its high mechanical properties (tensile strength of about 6 GPa) [18,19] and an appropriate bioactivity [13,20,21]. Both characteristics are very attractive for biomedical applications [22]. The particles of potassium polytitanate precursor used in this work have spherical shape with 20–30 μm in diameter [16] and they can be easily mixed with 45S5 Bioglass® powder and compacted by uniaxial pressing to obtain green bodies. The silicate glass transition temperature, $T_g \sim 550$ °C, and fluidization temperature, $T_f \sim 900$ °C [23–25], are appropriate to assist the crystallization of the potassium polytitanate and, due to this fact, composites can be obtained in a single stage.

In our previous work [26], mixtures of potassium polytitanate powder (10–30 wt.%) with powdered calcium-borate glass were prepared in order to obtain bioactive composites with improved mechanical properties by sintering at 800–900 °C. However, a relatively high release of boron to the simulated body fluid (SBF) was observed. This may lead to toxic effects. The target of this research is to obtain novel boron-free silicate glass-ceramics composites with high bioactivity, biocompatibility and appropriate mechanical properties.

II. Experimental

Bioglass® was prepared by the melt-quench method [27] using a batch of 28 $CaCO_3$, 25 $NaCO_3$, 13 $NH_4H_2PO_4$ and 34 SiO_2 in wt.% (Sigma Aldrich, USA). The raw materials mixture was placed into a platinum crucible and heated up to 1380 °C and kept at this temperature for 2 h. The obtained melt was quenched onto a stainless steel plate at room temperature. The glass was crushed and milled to obtain a powder with particle size between 45 and 150 μm. The potassium polytitanate (PP) precursor was prepared by heat treatment of a mixture consisting of TiO_2 powder (Anatase, Sigma Aldrich, 99%), KOH (Sigma Aldrich, 99%) and KNO_3 (Sigma Aldrich 98%) in a weight ratio of 1 : 1 : 8 at 500 °C for 2 h. Then, the product was washed with distilled water and dried at 60 °C for 4 h [16,17].

Composites were obtained by mixing Bioglass® powder with 20, 40, 60 or 80 wt.% of potassium polytitanate precursor. The composites obtained after sintering of these mixtures were identified as 20/80 SG, 40/60 SG, 60/40 SG and 80/20 SG (SG = silicate glass, 45S5 Bioglass®). Green bodies of the composites were produced by mechanical mixing and uniaxial pressing (160 MPa) to obtain flat disks of 1 cm in diameter and 0.5 cm in thickness for bioactivity and biocompatibility assays, and cylinders of 11 mm in height and 8 mm in diameter for compressive strength testing. The disks and cylinders were reactively sintered at 1000 °C for 1 h [9]. The sintered composites were analysed using X-ray diffraction (XRD, Philips PW3040) and scanning electron microscopy (SEM, Philips XL30, equipped with an energy dispersive spectroscopy analyser, EDS).

In vitro bioactivity assessment of composites was performed by immersing the samples in 250 ml of simulated body fluid (SBF-K9) at 37 °C for 21 days. The SBF used was prepared according to the literature [28] by dissolving reagent-grade chemicals of NaCl, $NaHCO_3$, KCl, $K_2HPO_4 \cdot 3H_2O$, $MgCl_2 \cdot 6H_2O$, $CaCl_2 \cdot 2H_2O$ and Na_2SO_4 in deionized water (1 dm^3) and buffered to pH 7.4 with tris(hydroxymethyl)-aminomethane and 1 N HCl at 37 °C. The surface of the samples was characterized by SEM, EDS and XRD. Cross-section analyses were also performed by using SEM and EDS.

The compressive strength of the composites was evaluated according to the ASTM C-773 standard. Tests were performed using a 15 kN capacity automated hydraulic machine (Controls, model 50-C7024). The reported strength was the average of six specimens of the same chemical composition.

In vitro cytotoxicity was assessed for the samples that showed higher bioactivity and appropriate compressive strength (20/80 SG and 40/60 SG). These assays, including adhesion tests, were performed according to the ISO 10993-5 standard using primary human osteoblasts (HOb). For this purpose, the selected samples were placed in a microbiological plate and then immersed in culture media during 24 h at physiological conditions (incubated at 37 °C in a humidified atmosphere of 5% CO_2 and 95% air). Each modified culture medium was extracted and placed in contact with a monolayer of freshly isolated human osteoblast-like cells during 24 h under the same conditions. After exposure time, the monolayer of cells was fixed and analysed using a commercial kit (Xenometrix, Germany), which allows the sequential evaluation of three different parameters for cell survival and integrity. The absorbance was evaluated using a UV-Vis microplate reader (Pow-

erWave MS2, BioTek Instruments, USA). The three parameters determined for each sample were mitochondrial activity (XTT), membrane integrity (Neutral Red - NR) and cell density (Crystal Violet Dye Elution - CVDE) [29,30]. Five replicas of these assays were performed.

Cell adhesion tests were performed using subcultures of human osteoblasts cells (12×10^4 cell/μl). These were seeded on the sintered samples and incubated at 37 °C in a humidified atmosphere of 5% CO_2 and 95% air. After 24 h, the samples were washed with phosphate buffer saline (PBS) and fixed with 4% para-formaldehyde during 15 min and washed 3 times with PBS. Finally, the samples were dried using diluted ethanol and exposed to a critical point drying under standard conditions (5% CO_2, 31.1 °C and 1072 psi). For analysis, the samples were coated with a gold layer and observed using a scanning electron microscope [31,32]. These assays were done in triplicate.

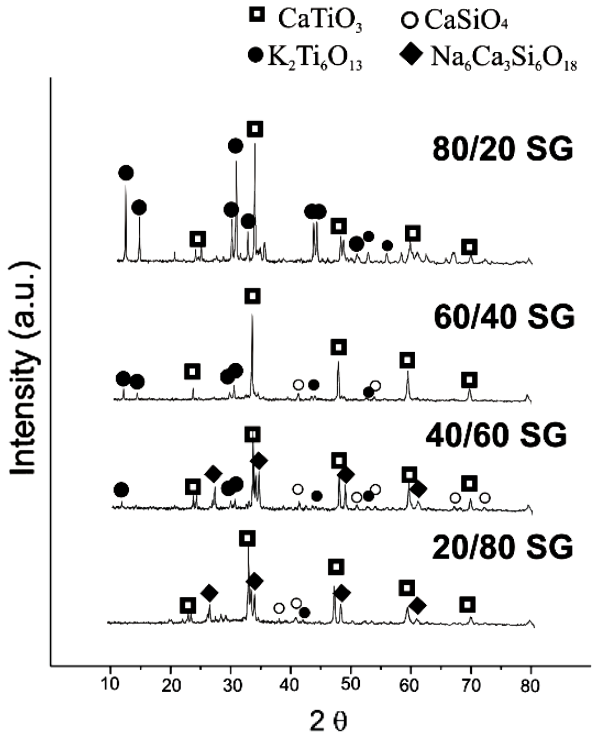

Figure 1. XRD patterns of composites obtained after reactive sintering at 1000 °C for 1 h

III. Results and discussion

The potassium polytitanate precursor synthesized by the molten salts method showed a TiO_2/K_2O ratio of 5.3, according to the energy dispersive spectroscopy analysis (EDS). This ratio is appropriate to obtain fibre-shaped potassium hexatitanate ($K_2Ti_6O_{13}$) during heat treatment [16,17].

The XRD patterns of the sintered composites are shown in Fig. 1. As observed, considerable changes occurred. The crystallization of the polytitanate precursor was identified. The crystalline phases that appeared in the products after reactive sintering were calcium silicate ($CaSiO_4$), sodium-calcium silicate ($Na_6Ca_3Si_6O_{18}$), potassium hexatitanate ($K_2Ti_6O_{13}$) and tetragonal calcium titanate ($CaTiO_3$). The calcium titanate obtained after reactive sintering suggests an intensive chemical interaction between the polytitanate precursor and 45S5 Bioglass® supported by a high ion exchange mobility of Ca and K cations. Amorphous phase was also detected, especially on those samples with high content of Bioglass®. The other observed phases were also obtained with the chemical reactions that occurred during sintering. As observed, potassium hexatitanate reflections are more intense when more than 40 wt.% of potassium polytitanate precursor was

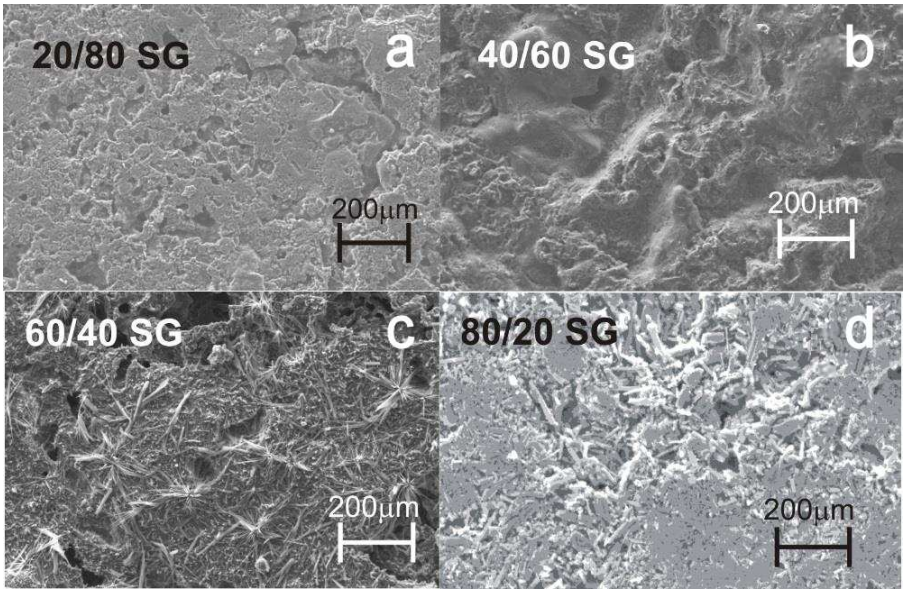

Figure 2. SEM images of composites obtained after reactive sintering at 1000 °C for 1 h: a) 20/80 SG, b) 40/60 SG, c) 60/40 SG and d) 80/20 SG

added to the raw materials mixture. The composites obtained when more than 60 wt.% of PP precursor was added show a high content of potassium hexatitanate and calcium titanate.

Figure 2 shows SEM images of the sintered composites. Those obtained when 60 or 80 wt.% of PP precursor was added, Figs 2c and 2d, respectively, show the formation of hexatitanate whiskers, which are not totally embedded into the matrix. This fact may lead to toxic materials, thus they are not attractive for biomedical applications. Nevertheless, the composites prepared with less than 60 wt.% of PP precursor presented a noticeable densification (20/80 SG and 40/60 SG, Figs. 2a and 2b, respectively).

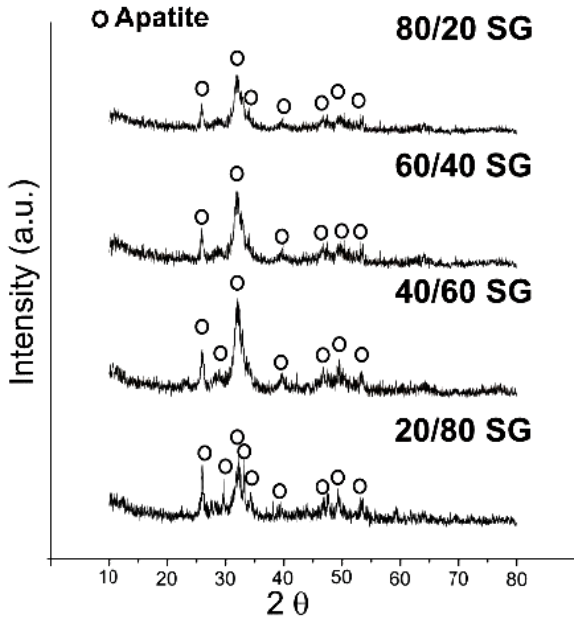

Figure 3. XRD patterns of composites after 21 days of immersion in SBF

Figure 3 shows the XRD patterns of the samples surface after 21 days of immersion in SBF. As observed, apatite was formed on the composites. These results indicate a high bioactivity of all the samples, since no peaks corresponding to the substrate were detected by XRD. This high bioactivity is due to the formation of Si–OH and Ti–OH groups on the surface in contact with SBF, which are preferential sites for apatite nucleation. Besides, the bioactivity of the potassium hexatitanate ($K_2Ti_6O_{13}$) has been reported earlier [13,20,22].

Figure 4 shows SEM images of the samples prepared by adding 20 and 40 wt.% of potassium polytitanate to the mixture, before and after 21 days of immersion in SBF. In both cases, before immersion, a high roughness surface, generated after sintering, was observed. The EDS spectrum corresponding to the matrix of the 40/60 sample (A) shows high intensity peaks of Ti and Ca. Some fibre-shaped potassium hexatitanate can be also observed at higher magnifications (B). These results are in agreement with those obtained by XRD (Fig. 1). After 21 days of immersion in SBF, the formed apatite layer, whose morphology closely resembles that formed on the highly bioactive materials, was observed on the 20/80 and 40/60 SG composites. The corresponding EDS spectrum (C) clearly indicates that this formed layer is rich in Ca and P with a Ca/P atomic ratio of 1.7, which is close to that of hydroxyapatite (1.67). Table 1 shows the chemical composition of the zones A, B and C.

The mechanism of apatite formation can be explained using cross-sectional SEM images and the corresponding EDS spectra of the samples prepared by adding 40 wt.% of potassium polytitanate precursor. In Fig. 5 it is possible to identify several layers with strong differences in chemical composition. The EDS spectrum corresponding to the Si-rich layer (identified with number 1) indicates the formation of silica gel com-

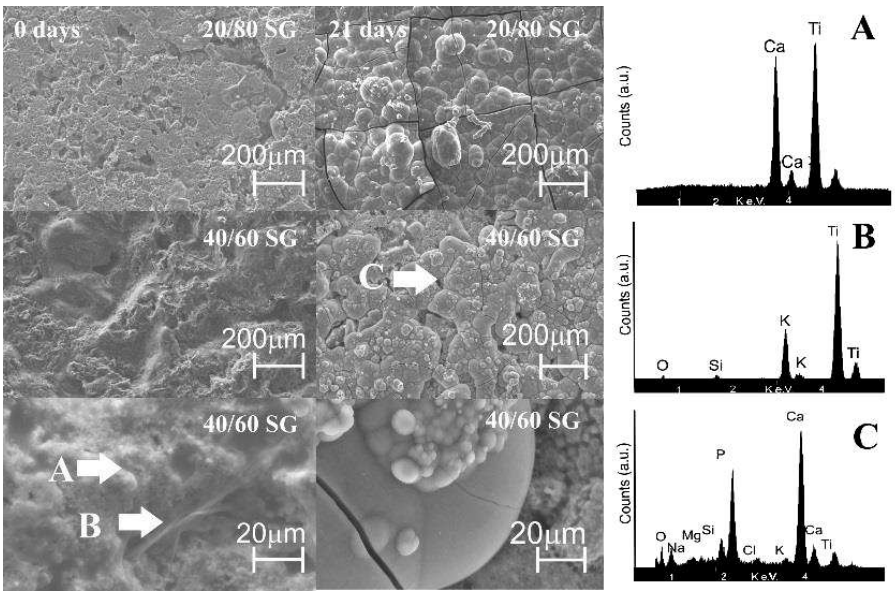

Figure 4. SEM images of 20/80 and 40/60 SG composites before (left) and after 21 days (right) of immersion in SBF (a) and EDS spectra corresponding to different regions of the 40/60 SG composite (b)

Table 1. EDS semiquantitative analyses of the different zones shown in Fig. 4

Zone ID	Chemical composition [at.%]									
	O	Na	Mg	Si	P	Cl	Ca	Ti	K	Ca/P
Calcium titanate (A)	26.9	1.84	-	1.65	-	-	29.67	38.16	1.78	-
Potassium titanate (B)	30.57	-	-	-	-	-	-	53.30	16.14	-
40/60 SG (C)	40.50	1.27	1.16	0.68	19.84	0.92	34.09	1.17	0.38	1.71

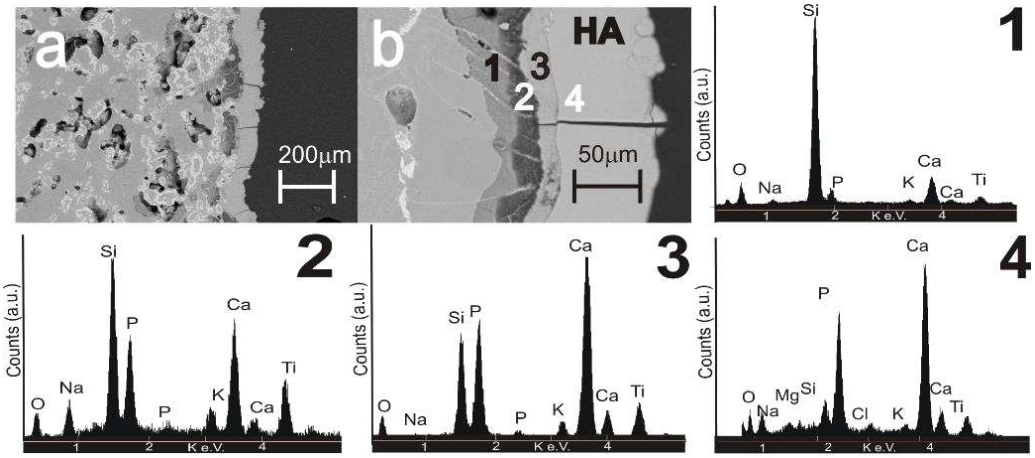

Figure 5. Cross-section SEM images of the 40/60 SG composite after 21 days of immersion in SBF at two different magnifications and EDS spectra corresponding to the indicated regions

monly formed on the existing bioactive systems (Si–OH groups). The second layer (layer number 2) is rich in Si, Ti, Ca and P, indicating that apatite is starting to form on the Si–OH and Ti–OH groups. The spectrum corresponding to the layer identified with number 3 indicates the growth of a Ca,P-rich compound as the intensity of Si and Ti peaks decreases while that of Ca and P increases. Finally, the thickest layer (4) corresponds to the apatite detected by XRD (Fig. 3). The EDS semiquantitative analysis of these Ca,P-rich layer (at.%) showed a Ca/P atomic ratio of 1.66, which is close to that of hydroxyapatite. These results demonstrate that the phases detected by XRD, calcium silicate ($CaSiO_4$), sodium-calcium silicate ($Na_6Ca_3Si_6O_{18}$), potassium hexatitanate ($K_2Ti_6O_{13}$) and the amorphous phase, play an important role in the formation of Si–OH and Ti–OH groups leading to a high bioactivity.

The compressive strength of the sintered composites (Fig. 6) decreases considerably when the polytitanate amount added to the mixtures is high (60/40 SG and 80/20 SG). This is due to the higher porosity obtained during the sintering (Fig. 2). In addition, when high quantities of polytitanate were added to the mixtures, the potassium hexatitanates fibres obtained during the heat treatment generated only few crisscrossed whiskers with no physical bond among them which are not enough to build a fibrous preform. On the other hand, when lower amounts of potassium polytitanate precursor (20/80 SG and 40/60 SG) were added, 45S5 Bioglass® acts like a bonding agent among the crystalline phases obtained during the sintering. These composites are very attractive for trabecular bone applications due to their appropriate compressive strength (35–50 MPa). The results obtained indicate that the mechanical properties of these composites are similar or even higher than those of some existing bioactive systems (5 to 20 MPa) [33]. Although compressive strength of these materials is lower than that of the calcium titanate/borosilicate glass composites reported earlier in our previous work [26], the potential toxic effects due to the presence of boron in the apatite layer is avoided.

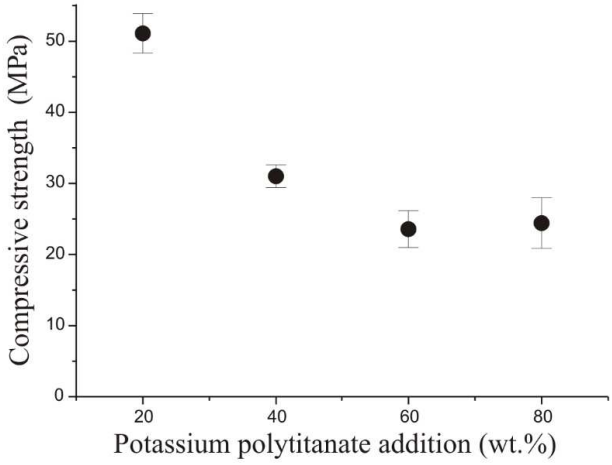

Figure 6. Compressive strength of SG composites

The mitochondrial activity (XTT test) was evaluated using cells treated with the modified culture media during 24 h by the bioactive composites. As it can be seen in Fig. 7 (XTT), the mitochondrial activity of cells in the modified media are not statistically different from the negative control (Cell). This indicates that mitochondrial activity is not disturbed by the modified media. The Neutral Red (NR) assay evaluates cellular integrity. As observed in Fig. 7 (NR) this assay showed that the cel-

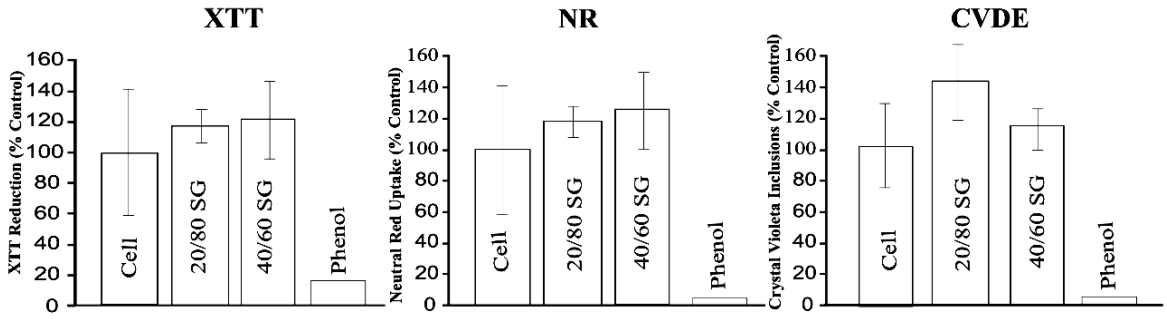

Figure 7. Cell viability assays (XTT, NR and CVDE) of the 20/80 SG and 40/60 SGb composites after 24 h of exposure

lular integrity continues to be viable after culturing for 24 h. No significant difference was observed between the modified media and the negative control (Cell). Cell density was evaluated by CVDE testing. Again, no significant difference was observed between the modified media and the negative control. This may be an indication that these composites are not cytotoxic. Statistical analyses were performed using F distribution, $p < 0.05$ (Minitab®18).

The results obtained from these assays indicate that the composites prepared in this work are biocompatible since all the modified media are considerably different from the positive control (phenol) and very similar to the osteoblast-like cells media.

An appropriate cell adherence to the substrates was observed in all the cases. In Fig. 8, corresponding to the cultured 20/80 and 40/60 SG composites, dense cell layers that coat the entire surfaces can be observed. At higher magnifications, the cell attachment is demonstrated.

IV. Conclusions

Novel bioactive and biocompatible composites can be obtained from powder mixtures of potassium polytitanate precursor and 45S5 Bioglass®. After reactive sintering, highly bioactive composites with appropriate compressive strength (35–50 MPa) were obtained. The compressive strength of the composite with 20 wt.% of potassium polytitanate precursor is about 60% higher than that with 40 wt.%. Mechanism of apatite formation was elucidated analysing the several layers formed after immersion of the samples in SBF. Apatite nucleates preferentially on Si and Ti-rich phases. The composites obtained with 20 or 40 wt.% of potassium polytitanate precursor, demonstrated an appropriate compres-

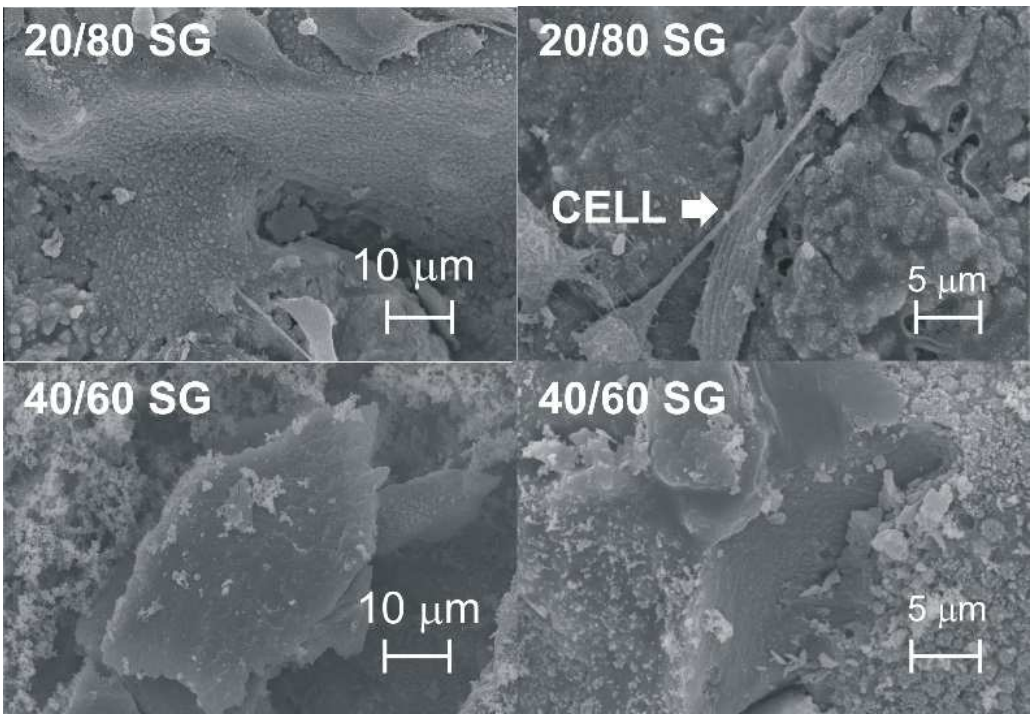

Figure 8. SEM images of the 20/80 and 40/60 SG composites after 24 h of culturing at different magnifications

sive strength and they were non-cytotoxic. The obtained results indicate that such composites are potential materials for hard tissue regeneration.

References

1. E. Verne, R. Defilippi, G. Carl, C. Vitale Brovarone, P. Appendino, "Viscous flow sintering of bioactive glass-ceramic composites toughened by zirconia particles", *J. Eur. Ceram. Soc.*, **23** (2003) 675–683.
2. L.-C. Gerhardt, A. Boccaccini, "Bioactive glass and glass-ceramic scaffolds for bone tissue engineering", *Materials*, **3** (2010) 3867–3910.
3. M.N. Rahaman, D.E. Day, B.S. Bal, Q. Fu, S.B. Jung, L.F. Bonewald, A.P. Tomsia, "Bioactive glass in tissue engineering", *Acta Biomater.*, **7** (2011) 2355–2373.
4. H.B. Guo, X. Miaoa, Y. Chen, P. Cheang, K.A. Khor, "Characterization of hydroxyapatite- and bioglass-316L fiber composites prepared by spark plasma sintering", *Mater. Lett.*, **58** (2004) 304–307.
5. S. Bharathi, Ch. Soundarapandian, D. Basu, S. Datta, "Studies on a novel bioactive glass and composite coating with hydroxyapatite on titanium based alloys: Effect of γ-sterilization on coating", *J. Eur. Ceram. Soc.*, **29** (2009) 2527–2535.
6. *Engineered Materials Handbook Volume 4: Ceramics and Glasses*, ASM International, USA, 1991.
7. I. Becker, I. Hofmann, F.A. Muller, "Preparation of bioactive sodium titanate ceramics", *J. Eur. Ceram. Soc.*, **27** (2007) 4547–4553.
8. X. Chen, Y. Li, P. D. Hodgson, C. Wen, "The importance of particle size in porous titanium and nonporous counterparts for surface energy and its impact on apatite formation", *Acta Biomater.*, **5** (2009) 2290–2302.
9. H.H. Beherei, K.R. Mohamed, G.T. El-Bassyouni, "Fabrication and characterization of bioactive glass (45S5)/titania biocomposites", *Ceram. Int.*, **35** (2009) 1991–1997.
10. T. Kokubo, T. Matsushita, H. Takadama, "Titania-based bioactive materials", *J. Eur. Ceram. Soc.*, **27** (2007) 1553–1558.
11. D.J. Haders, A. Burukhin, Y. Huang, D.J.H. Cockayne, R.E. Riman, "Phase-sequenced deposition of calcium titanate/hydroxyapatite films with controllable crystallographic texture onto Ti6Al4V by triethyl phosphate-regulated hydrothermal crystallization", *Cryst. Growth Des.*, **9** [8] (2009) 3412–3422.
12. N. Ohtsu, Ch. Abe, T. Ashino, S. Semboshi, K. Wagatsuma, "Calcium-hydroxide slurry processing for bioactive calcium-titanate coating on titanium", *Surf. Coat. Tech.*, **202** (2008) 5110–5115.
13. X. Wang, Sh. J. Liu, Y.M. Qi, L. Ch. Zhao, Ch. X. Cui, "Behavior of potassium titanate whisker in simulated body fluid", *Mater. Lett.*, **135** (2014) 139–142.
14. Sh. Wu, X. Liu, T. Hu, Y. Ho, "A biomimetic hierarchical scaffold: natural growth of nanotitanates on three dimensional micro porous Ti-based metals", *Nano Lett.*, **8** [11] (2008) 3803–3808.
15. A.V. Gorokhovsky, D.A. Cortes-Hernandez, N.N. Shcherbakova, "Composites from mixtures of potassium polytitanate and biocompatible glasses", *Glass Ceram.*, **67** (2011) 358–360.
16. T. Sanchez-Monjaras, A. Gorokhovsky, J.I. Escalante-García, "Molten salt synthesis and characterization of potassium polytitanate ceramic precursors with varied TiO_2/K_2O molar ratios", *J. Am. Ceram. Soc.*, **91** (2008) 3058–3065.
17. A.V. Gorokhovsky, J.I. Escalante-García, T. Sánchez-Monjarás, C.A. Gutiérrez-Chavarría, "Synthesis of potassium polytitanate precursors by treatment of TiO_2 with molten mixtures of KNO_3 and KOH", *J. Eur. Ceram. Soc.*, **24** (2004) 3541–3546.
18. N. Bao, X. Feng, X. Lu, Z. Yang, "Study on the formation and growth of potassium titanate whiskers", *J. Mater. Sci.*, **37** (2002) 3035–3043.
19. D.Y. Ding, J.N. Wang, "Interfacial reactions in $K_2Ti_6O_{13}$ whisker/Al_2O_3/Al composite", *Mater. Sci. Technol.*, **17** [7] (2001) 833–836.
20. Y. Liu, K. Tsuru, S. Hayakawa, A. Osaka, "Potassium titanate nanorod arrays grown on titanium substrate and their in vitro bioactivity", *J. Ceram. Soc. Jpn.*, **112** [2] (2004) 634–640.
21. Q. Liu, Y. Liu, T. Lei, Y. Tan, H. Wu, J. Li, "Preparation and characterization of nanostructured titanate bioceramic coating by anodization-hydrothermal method", *Appl. Surf. Sci.*, **328** (2015) 279–286.
22. Z. Zhao, X. Chen, A. Chen, G. Huo, H. Li, "Preparation of $K_2Ti_6O_{13}/TiO_2$ bioceramic on titanium substrate by micro-arc oxidation", *J. Mater. Sci.*, **44** (2009) 6310–6316.
23. Q.Z. Chena, I.D. Thompson, A.R. Bocaccini, "45S5 Bioglasss-derived glass-ceramic scaffolds for bone tissue engineering", *Biomaterials*, **27** (2006) 2414–2425.
24. P.N. De Aza, A.H. De Aza, P. Peña, S. De Aza, "Bioactive glasses and glass-ceramics", *Bol. Soc. Esp. Ceram. V.*, **46** [2] (2007) 45–55.
25. L.L. Hench, "Bioceramics", *J. Am. Ceram. Soc.*, **81** [7] (1998) 1705–1728.
26. A. Villalpando-Reyna, D.A. Cortés-Hernández, A. Gorokovsky, J.M. Almanza-Robles, J.C. Escobedo-Bocardo, "In vitro bioactivity assessment and mechanical properties of novel calcium titanate/borosilicate glass composites", *Ceram. Int.*, **37** (2011) 1625–1629.
27. H.M.M. Moawad, H. Jain, "Creation of nano-macro-interconnected porosity in a bioactive glass-ceramic by the melt-quench-heat-etch method", *J. Am. Ceram. Soc.*, **90** [6] (2007) 1934–1936.
28. T. Kokubo, H. Kuchitaniand, S. Sakka, T. Kitsugi, T. Yamamuro, "Solution able to reproduce in vivo surface structure changes in bioactive glass ceramic A-W", *J. Biomed. Mater. Res.*, **24** (1990) 721–734.
29. M.Z. Scelza, A.B. Linhares, L.E. Da Silva, J.M. Granjeiro, G.G. Alves, "A multiparametric assay to compare the cytotoxicity of endodontic sealers with primary human osteoblasts", *Int. Endod. J.*, **45** (2012) 12–18.
30. I.R. De Lima, G.G. Alves, C.A. Soriano, A.P. Campaneli, T.H. Gasparoto, E.S. Jr. Ramos, L.Á. De Sena, A.M. Rossi, J.M. Granjeiro, "Understanding the impact of divalent cation substitution on hydroxyapatite: An in vitro multiparametric study on biocompatibility", *J. Biomed. Mater. Res. A*, **98** [3] (2011) 351–358.
31. K. Anselme, P. Davidson, A.M. Popa, M. Giazzon, M. Liley, L. Ploux, "The interaction of cells and bacteria with surfaces structured at the nanometre scale", *Acta Biomater.*, **6** (2011) 3824–3846.
32. A. Zareidoost, M. Yousefpour, B. Ghaseme, A. Amanzadeh, "The relationship of surface roughness and cell re-

sponse of chemical surface modification of titanium", *J. Mater. Sci. Mater. Med.*, **23** [6] (2012) 1479–1488.
33. Q. Fu, E. Saiz, M. N. Rahaman, A.P. Tomsia, "Bioactive glass scaffolds for bone tissue engineering: state of the art and future perspectives – a review", *Mater. Sci. Eng. C*, **31** (2011) 1245–1256.